J|A|C|S
ARTICLES
Published on Web 04/22/2004

Proton Inventory Studies of α-Thrombin-Catalyzed Reactions of Substrates with Selected P and P′ Sites

Edith J. Enyedy and Ildiko M. Kovach*

Contribution from the The Catholic University of America, Chemistry Department, Washington D.C. 20064

Received December 31, 2003; E-mail: kovach@cua.edu

Abstract: Deuterium kinetic solvent isotope effects for the human α-thrombin-catalyzed hydrolysis of (1) substrates with selected P_1-P_3 sites, *Z*-Pro-Arg-7-amido-4-methylcoumarin (7-AMC), *N-t*-Boc-Val-Pro-Arg-7-AMC, Bz-Phe-Val-Arg-4-nitroanilide (pNA), and *H*-D-Phe-L-Pip-Arg-pNA, are $^{DOD}k_{cat} = (2.8-3.3) \pm 0.1$ and $^{DOD}(k_{cat}/K_m) = (0.8-2.1) \pm 0.1$ and (2) internally fluorescence-quenched substrates (a) (AB)Val-Phe-Pro-Arg-Ser-Phe-Arg-Leu-Lys(DNP)-Asp-OH, an optimal sequence, and (b) (AB)Val-Ser-Pro-Arg-Ser-Phe-Gln-Lys(DNP)-Asp-OH, recognition sequence for factor VIII, are $^{DOD}k_{cat} = 2.2 \pm 0.2$ and $^{DOD}(k_{cat}/K_m) = (0.8-0.9) \pm 0.1$, at the pL (L = H, D) maximum, 8.4−9.0, and (25.0−26.0) ± 0.1 °C. The most plausible models fitting the partial isotope effect (proton inventory) data have been selected on the basis of lowest values of the reduced chi squared and consistency of fractionation factors at all substrate concentrations, assuming rate-determining acylation. The data for *Z*-Pro-Arg-7-AMC are consistent with a single-proton bridge at the transition state $\phi^{TS} = 0.39 \pm 0.05$ and components for solvent reorganization $\phi_S = 0.8 \pm 0.1$ and $\phi_S = 1.22$ for k_{cat} and k_{cat}/K_m, respectively. The data for tripeptide amides fit bowl-shaped curves; an example is *N-t*-Boc-Val-Pro-Arg-7-AMC: $\phi^{TS}_1 = \phi^{TS}_2 = 0.57 \pm 0.01$ and $\phi_S = 1$ for k_{cat} and 1.6 ± 0.1 for k_{cat}/K_m. Proton inventories for the nonapeptide (2b) are linear. The data for k_{cat} for *H*-D-Phe-L-Pip-Arg-pNA and the decapeptide (2a) are most consistent with two identical fractionation factors for catalytic proton bridging, $\phi^{TS}_1 = \phi^{TS}_2 = 0.68 \pm 0.02$ and a large inverse component ($\phi_S = 3.1 \pm 0.5$) for the latter, indicative of substantial solvent reorganization upon leaving group departure. Proton inventory curves for k_{cat}/K_m for nearly all substrates are dome-shaped with an inverse isotope effect component ($\phi_S = 1.2-2.4$) originating from solvent reorganization during association of thrombin with substrate. These large contributions from medium effects are in full accord with the conformational adjustments required for the fulfillment of the dual, hemostatic and thrombolytic, functions of thrombin.

Introduction

The key element in serine hydrolase catalysis is the acid−base machinery.[1−5] A basic tenet of enzymic acid−base catalysis is that the occurrence of the proton bridges at active sites is most pertinent in transition state (TS) stabilization.[6] The free energy of this stabilization of the TS is estimated to be 5−10 kcal/mol for a number of hydrolases.[7−10] Arguably, deuterium (tritium) isotope effects, i.e., deuterium kinetic solvent isotope effects (KSIEs) in the case of enzymic reactions, are the best measures of the nature of proton transfer in general acid−base-catalyzed reactions.[3,4,11−13] Proton inventories are an extension of the solvent isotope effect method reporting predominantly on the number and, to some extent, the nature of proton bridges at TSs.[3,4,11−19] Since the 1980s, R. L Schowen and his associates[3,4,11,13,15,17] employed the proton inventory method to probe the hypothesis that subsites on peptide substrates exert a

(1) Polgar, L. *Mechanisms in Protease Action*; CRC Press: Boca Raton, FL, 1990; pp 87−113.
(2) Hedstrom, L. *Chem. Rev.* **2002**, *102*, 159−177.
(3) Schowen, R. L. Structural and Energetic Aspects of Protolytic Catalysis by Enzymes: Charge−Relay Catalysis in the Function of Serine Proteases. In *Mechanistic Principles of Enzyme Activity*; Liebman, J. F., Greenberg, A., Eds.; VCH Publishers: New York, 1988; pp 119−168.
(4) Schowen, K. B.; Limbach, H. H.; Denisov, G. S.; Schowen, R. L. *Biochim. Biophys. Acta.* **2000**, *1458*, 43−62.
(5) Fersht, A. *Structure and Mechanism in Protein Science*; W. H. Freeman and Co.: New York, 1999; pp 1−631.
(6) Schowen, R. L. Catalytic Power and Transition-State Stabilization. In *Transition States of Biochemical Proceses*; Gandour, R. D., Schowen, R. L., Eds.; Plenum: New York, 1978; pp 77−114.
(7) Frey, P. A.; Whitt, S. A.; Tobin, J. B. *Science* **1994**, *264*, 1927−1930.
(8) Cleland, W. W.; Kreevoy, M. M. *Science* **1994**, *264*, 1887−1890.
(9) Scheiner, S.; Kar, T. *J. Am. Chem. Soc.* **1995**, *117*, 6970−6975.
(10) Ash, E. L.; Sudmeier, J. L.; De Fabo, E. C.; Bachovchin, W. W. *Science* **1997**, *278*, 1128−1132.
(11) Alvarez, F. J.; Schowen, R. L. Mechanistic Deductions from Solvent Isotope Effects. In *Isotopes in Organic Chemistry*; Buncel, E., Lee, C. C., Eds.; Elsevier: Amsterdam, 1987; pp 1−60.
(12) Kresge, A. J.; More, O.; Powell, M. F. Solvent Isotopes Effects, Fractionation Factors and Mechanisms of Proton-Transfer Reactions. In *Isotopes in Organic Chemistry*; Buncel, E., Lee, C. C., Eds.; Elsevier: Amsterdam, 1987; pp 177−273.
(13) Quinn, D. M.; Sutton, L. D. Theoretical Basis and Mechanistic Utility of Solvent Isotope Effects. In *Enzyme Mechanism from Isotope Effects*; Cook, P. F., Ed.; CRC Press: Boston, MA, 1991; pp 73−126.
(14) Elrod, J. P.; Hogg, J. L.; Quinn, D. M.; Schowen, R. L. *J. Am. Chem. Soc.* **1980**, *102*, 5365−5376.
(15) Venkatasubban, K. S.; Schowen, R. L. *CRC Crit. Rev. Biochem.* **1985**, *17*, 1−44.
(16) Stein, R. L.; Elrod, J. P.; Schowen, R. L. *J. Am. Chem. Soc.* **1983**, *105*, 2446−2452.
(17) Stein, R. L.; Strimpler, A. M.; Hori, H.; Powers, J. C. *Biochemistry* **1987**, *26*, 1305−1314.
(18) Scholten, J. D.; Hogg, J. L.; Raushel, F. M. *J. Am. Chem. Soc.* **1988**, *110*, 8246−8247.
(19) Chiang, Y.; Kresge, A. J.; Chang, T. K.; Powell, M. F.; Wells, J. A. *J. Chem. Soc., Chem. Commun.* **1995**, 1587−1588.

Scheme 1. Double Displacement Mechanism of Serine Protease Catalysis of Peptide Hydrolysis

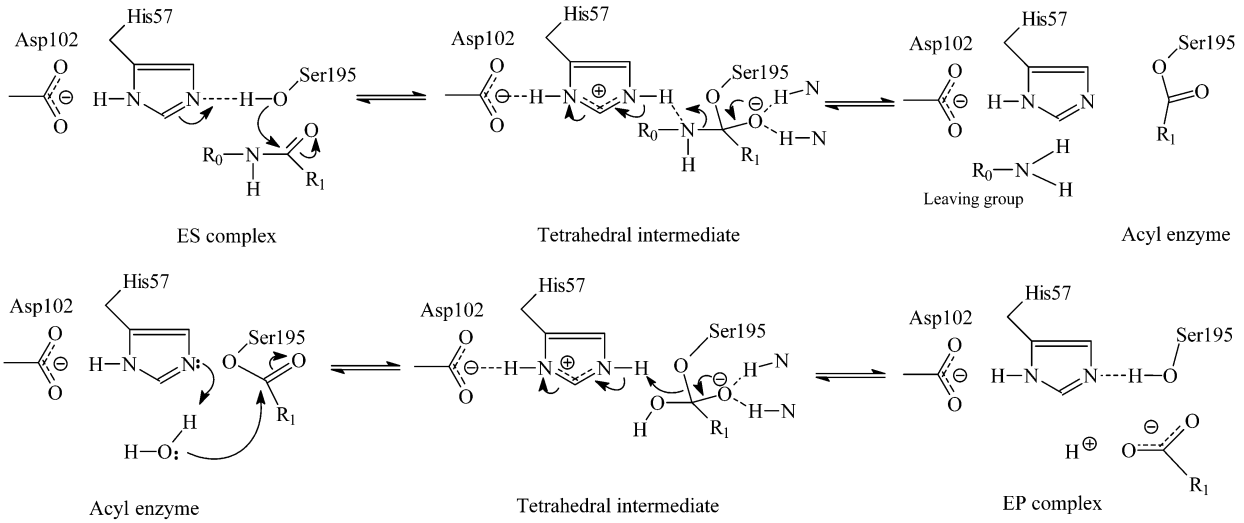

degree of compression to elicit contraction of the distance between proton donors and acceptors in acid−base catalytic pairs at the active site of enzymes. This in turn adjusts and optimizes the p*K* of the attacking nucleophile as it forms the covalent bond to the carbonyl C.[20] It has been demonstrated that the compression is exerted at P subsites in rationally selected peptide substrates[21,22] and inhibitors.[17] In more recent years, P. A. Frey's group[7,23−26] and others[10,27−29] have provided new supportive evidence for the importance of contracting the distances across hydrogen-bond donors and acceptors at active sites, by measuring H NMR signals of short strong hydrogen bonds (SSHBs) in proteases modified by transition-state analogues. Other studies with substrates and inhibitors indicated that P′ sites[30−33] and exosites[34] in long peptide/protein substrates may have a similar role. Cardiovascular proteases are uniquely suitable for studying these effects, because they are enzymes of great specificity and contain exosites, beyond the S and S′ sites, critical for their function.[34−36] Good techniques exist for studying them with appropriate substrates.

Catalytic Mechanism of Peptide Hydrolysis by α-Thrombin. α-Thrombin is the most selective and multifunctional of the 13 serine proteases recruited in blood clotting; it plays a role in both hemostasis and thrombolysis.[34−39] It is also a remarkably efficient serine protease in terms of catalytic acceleration of the hydrolysis of substrates that fulfill the requirements for specificity.[39−41] The obligatory scissile bond for thrombin-catalyzed hydrolysis is Arg-Ser, but Arg-Gly and Arg-Val are also cleaved with less efficiency. Thrombin shares with other serine proteases (hydrolases) a unique combination of catalytic features: the catalytic triad (Ser[195], His[57], and Asp[102]), the oxyanion hole, and the specificity-binding S_1 site. It also has S′ sites and at least two exo binding sites for its large substrates, fibrinogen, proteins C, regulatory proteins, and cofactors.[34,42] While the presence and location of binding subsites vary among the members of serine hydrolases, they all perform the task of nucleophilic displacement at carbonyl by a double displacement mechanism, shown in detail in Scheme 1.[3,5]

Scheme 2

$$E + S \underset{}{\overset{K_{as}}{\rightleftharpoons}} ES \xrightarrow{k_2} P_1 + EP \xrightarrow{k_3} E + P_2$$

The His[57]-catalyzed nucleophilic attack of Ser[195] resulting in the formation of a tetrahedral intermediate and the ensuing $His^{57}H^+$-catalyzed cleavage of the C−N bond are key to serine hydrolase catalysis. Proton transfer in these general acid−base-catalyzed steps may be mediated by an SSHB at the TS.[4] Each of these steps can be assisted by the formation of a hydrogen bridge between the carboxylate of Asp[102] and the imidazole of His[57] accepting the positive charge. The deacylation phase is the repeat of these steps, but with water as nucleophile to result in the hydrolysis of the acyl enzyme. The major steps are outlined in Scheme 2.

In general, Michaelis−Menten kinetics is observed, and the constants can be defined in terms of elementary rate constants as follows: $k_{cat}/K_m = k_1k_2k_3/(k_{-1}k_2 + k_{-1}k_3 + k_2k_3)$ and $k_{cat} =$

(20) García-Viloca, M.; González-Lafont, A.; Luch, J. M. *J. Phys. Chem.* **1997**, *101*, 3880−3886.
(21) Stein, R. L. *J. Am. Chem. Soc.* **1983**, *105*, 5111−5116.
(22) Stein, R. L.; Strimpler, A. M. *J. Am. Chem. Soc.* **1987**, *109*, 4387−4390.
(23) Tobin, J. B.; Whitt, S. A.; Cassidy, C. S.; Frey, P. A. *Biochemistry* **1995**, *34*, 6919−6924.
(24) Cassidy, C. S.; Lin, J.; Frey, P. A. *Biochemistry* **1997**, *36*, 4576−4584.
(25) Lin, J.; Westler, W. M.; Cleland, W. W.; Markley, J. L.; Frey, P. A. *Proc. Natl. Acad. Sci. U.S.A.* **1998**, *95*, 14664−14668.
(26) Lin, J.; Cassidy, C. S.; Frey, P. A. *Biochemistry* **1998**, *37*, 11940−11948.
(27) Halkides, C. J.; Wu, Y. Q.; Murray, C. J. *Biochemistry* **1996**, *35*, 15941−15948.
(28) Kahayaoglu, A.; Haghjoo, K.; Guo, F.; Jordan, F.; Kettner, C.; Felfoldi, F.; Polgar, L. *J. Biol. Chem.* **1997**, *272*, 25547−25554.
(29) Bao, D.; Huskey, P. W.; Kettner, C. A.; Jordan, F. *J. Am. Chem. Soc.* **1999**, *121*, 4684−4689.
(30) Schellenberger, V.; Turck, C. W.; Hedstrom, L.; Rutter, W. J. *Biochemistry* **1993**, *32*, 4349−4353.
(31) Schellenberger, V.; Turck, C. W.; Rutter, W. J. *Biochemistry* **1994**, *33*, 4251−4257.
(32) Dai, Y.; Hedstrom, L.; Abeles, R. H. *Biochemistry* **2000**, *39*, 6498−6502.
(33) Le Bonniec, B. F.; Myles, T.; Johnson, T.; Knight, C. G.; Tapparelli, C.; Stone, S. R. *Biochemistry* **1996**, *35*, 7114−7122.
(34) Berliner, L. J. *Thrombin: Structure and Function*; Plenum Press: New York, 1992; pp 63−438.
(35) Mann, K. G.; Lorand, L. *Methods Enzymol.* **1993**, *222*, 1−10.
(36) Davie, E. W.; Fujikawa, K.; Kisiel, W. *Biochemistry* **1991**, *29*, 10363−10370.
(37) Furie, B.; Furie, B. C. *Cell* **1988**, *53*, 505−518.
(38) Patthy, L. *Methods Enzymol.* **1993**, *222*, 10−22.
(39) Dang, Q. D.; Vindigni, A.; Di Cera, E. *Proc. Natl. Acad. Sci. U.S.A.* **1995**, *92*, 5977−5981.
(40) Stone, S. R.; Betz, A.; Hofsteenge, J. *Biochemistry* **1991**, *30*, 9841−9848.
(41) Vindigni, A.; Di Cera, E. *Biochemistry* **1996**, *35*, 4417−4426.
(42) Bode, W.; Mayr, I.; Baumann, U.; Huber, R.; Stone, S. R.; Hofsteenge, J. *EMBO J.* **1989**, *8*, 3467−3475.

$k_2k_3/(k_2 + k_3)$. The first step of the scheme is reversible substrate binding ($K_{as} = k_1/k_{-1}$) followed by acylation (k_2) and deacylation (k_3). The proton-transfer steps, shown in Scheme 1, coupled or uncoupled to bond making and breaking, are critical in the elucidation of the mechanisms of action of these enzymes.[3,4]

The main goal of this project has been to characterize the number of protonic sites and their mode of participation in the catalysis of substrate hydrolysis by human α-thrombin, using the proton inventory technique. We investigated full and partial KSIEs for human α-thrombin-catalyzed hydrolysis of substrates for an understanding of protonic participation as recruited at S and S′ specific subsites. S′ subsites have recently been the target of many investigations, and thus, it seemed timely to inquire into their importance in the mobilization of protonic bridges at the TS and solvent reorganization in a key enzyme catalyzing the hydrolysis of relevant substrates. Substrates are two types: (1) chromogenic or fluorogenic di- to tripetide amide substrates test the effect of P_1-P_3 residues, *Z*-Pro-Arg-7-amido-4-methylcoumarin (PR-AMC), *N*-*t*-Boc-Val-Pro-Arg-7-AMC (VPR-AMC), Bz-Phe-Val-Arg-4-nitroanilide (FVR-pNA), and *H*-D-Phe-L-Pip-Arg-pNA (FPiR-pNA); (2) fluorescence-quenched substrates with an N-terminal 2-aminobenzoyl (AB)-Val fluorophore, a C-terminal Lys-2,4-dinitrophenyl (DNP) quencher, and an Asp-OH to enhance solubility such as (AB)Val-Phe-Pro-Arg-Ser-Phe-Arg-Leu-Lys(DNP)-Asp-OH, (scissile bond and flanking sequences, FPR-SFR) the optimal substrate,[33] and (AB)Val-Ser-Pro-Arg-Ser-Phe-Gln-Lys(DNP)-Asp-OH, (scissile bond and flanking sequences PR-SF) the recognition sequence for factor VIII, to test the collective contribution of P_1-P_5 and $P_1'-P_5'$ sites, but without exosites. We interpret the one- or two-proton bridges identified in the rate-determining step of these reactions according to the "alternate" model of Schowen, i.e., not being part of the reaction coordinate.[4] An important outcome of this work is that all KSIEs on enzyme−substrate association steps and leaving group dissociation steps contain an inverse solvent isotope effect component, for hydrogen bonds at sites of solvation.

Experimental Section

Materials. Anhydrous *N*,*N*-dimethyl sulfoxide (DMSO), anhydrous *N*,*N*-dimethyl formamide (DMF), heavy water with 99.9% deuterium content, and anhydrous methanol were purchased from Aldrich Chemical Co.. All buffer salts were reagent grade and were purchased from Aldrich, Fisher, or Sigma Chemical Co.. Solid 4-methyl umbelliferyl guanidinobenzoate (MUGB) hydrochloride, 4-methyl umbelliferone (4-MU), *N*-*t*-Boc-Val-Pro-Arg 7-AMC hydrochloride, and Bz-Phe-Val-Arg-4-nitroanilide (pNA) > 99% pure (TLC) were purchased from Sigma Chemical Co.. *Z*-Pro-Arg-7-AMC acetate > 98% pure (TLC) was purchased from Bachem CA Inc., and *H*-D-Phe-Pip-Arg-pNA 99% (TLC) was purchased from Diapharma Group Inc.. (AB)Val-Phe-Pro-Arg-Ser-Phe-Arg-Leu-Lys(DNP)-AspOH and (AB)Val-Ser-Pro-Arg-Ser-Phe-Gln-Lys(DNP)-AspOH were >95% pure (HPLC) custom synthesized by BioSynthesis Inc. (Lewisville, TX). Mass-spectral analysis confirmed their molecular mass, 1550 d and 1349 d, respectively. Human α-thrombin, MM 36 500 d and 3010 NIH u/mg activity in pH 6.5, 0.05 M sodium citrate buffer, 0.2 M NaCl, 0.1% PEG-8000, was purchased from Enzyme Research Laboratories.

Active-Site Concentrations. MUGB in pH 8.05, 0.05 M sodium barbital, 0.10 M NaCl, 0.1% PEG-4000 in at least 200-fold excess over thrombin, was used. The stoichiometric release of 4-MU was recorded in the concentration range 0−30 nM for 6 min in 2 s intervals. The background hydrolysis of MUGB in the assay buffer was recorded in advance for the same time period. The intercept given by a linear fit of a section of the intensity dependence on time for >180 s gave the concentration of thrombin. Alternatively, initial velocity measurements of fluorescence during hydrolysis of *N*-*t*-Boc-Val-Pro-Arg 7-AMC were carried out. The substrate concentration in the cuvette ranged from 1.7 to 18.6 μM, and the average enzyme concentration in the cuvette was 3.6 nM. There was no background hydrolysis of the substrate in the absence of enzyme, and the slopes were proportional to thrombin concentration.

Solutions. Buffers were prepared by weight from Tris-base and Tris-HCl in the range pH 7.1−9.1 in freshly distilled deionized water or heavy water to contain 0.02 M Tris, 0.3 M NaCl, or choline chloride (ChCl) and 0.1% PEG-4000. The density of the two buffer stock solutions in water and heavy water was determined at room temperature. Buffers in isotopic mixtures of water were prepared by volumetric mixing. The fraction of deuterium in every buffer was carefully calculated, accounting for density, mass of the enzyme stock solution, and presence of buffer salts. The pure D_2O buffer was stored over dry silicagel. The pH was measured using a Fisher pH combination electrode and the PhM84 radiometer electronic readout. Temperature corrections were applied to Tris buffers according to ($dpK_a/dt = -0.027$). The pD was calculated by adding 0.4 to the electrode reading.

MUGB was stored in 0.5 mM stock solution in 0.001 M HCl. Substrate stock solutions in anhydrous DMSO were as follows: *Z*-Pro-Arg-7-AMC 90 mM, *N*-*t*-Boc-Val-Pro-Arg 7-AMC 12 mM, Bz-Phe-Val-Arg-pNA 19.5 mM, and *H*-D-Phe-Pip-Arg-pNA 3.2 mM. The exact concentration of the substrate was determined after thrombin-catalyzed hydrolysis, by measuring the fluorescence of released 7-AMC or measuring the absorption increase at 400 nm for pNA release from 4-nitroanilide substrates, in a known volume of the initial substrate. DMSO stock solutions of the nona- and decapeptides were 19.6 mM for (AB)Val-Phe-Pro-Arg-Ser-Phe-Arg-Leu-Lys(DNP)-Asp-OH and 49.5mM for (AB)Val-Ser-Pro-Arg-Ser-Phe-Gln-Lys(DNP)-AspOH and were stored in a desiccated jar at −20 °C.

Instruments. Spectroscopic measurements were performed with either a Perkin-Elmer Lambda 6 or Lambda 7 UV−vis spectrophotometer connected to a PC. Fluorometric measurements were performed using an SLM-Aminco SPF-500C spectrofluorometer connected to a PC. The excitation and emission wavelengths were 365 and 445 nm, respectively, for 4-MU and 7-AMC. A range up to 0.970−1.030 for the fluorescence ratio reading was defined by preparing a calibration solution of 4-MU or 7-AMC (2 μM) of known concentration and raising the high voltage of the emission photomultiplier until a reading close to 1 was reached. The concentration of the calibration solution was a function of the concentration of 4-MU or 7-AMC expected to be released during the enzyme assays. When intramolecularly quenched substrates were used, the excitation wavelength was $\lambda_{ex} = 325$ nm and the emission wavelength was $\lambda_{em} = 420$ nm.

The temperature was monitored using a temperature probe connected to a digital readout device. Either a Neslab RTE-4 or a Lauda 20 circulating water bath was used for temperature control. Positive displacement Gilson and Rainin Microman pipets with plastic tips were used for the delivery of enzyme solution, substrate solution, and organic solvent.

Fluorescence Quenching. Fluorescence quenching of 7-AMC by high substrate concentration was measured at 0, 45, 90, 270, and 450 μM *Z*-Pro-Arg-7-AMC by adding 50 μL increments of 15.4 μM 7-AMC solution to 2.00 mL of pH 8.43 Tris buffer at 26.0 ± 0.1 °C. Fully hydrolyzed substrate was used to determine quenching of the released products by (AB)Val-Ser-Pro-Arg-Ser-Phe-Gln-Lys(DNP)-Asp-OH. Aliquots of 2 μL of a 522 μM hydrolyzed substrate were added to 0, 11.7, 23.3, 34.4, 53.8, 63.7, and 73.5 μM (AB)Val-Ser-Pro-Arg-Ser-Phe-Gln-Lys(DNP)-Asp-OH solutions, and the fluorescence was recorded at 25.0 ± 0.1 °C and in isotopic buffers at $n = 0$, 0.09, 0.49, 0.89, and 1.00.

Table 1. Michaelis−Menten Constants for the Human α-Thrombin-Catalyzed Hydrolysis of Peptide-AMC, Internally Fluorescence-Quenched Peptides, and Peptide-pNA Substrates at pH 8.4−8.6, 0.02 M Tris, 0.3 M NaCl, 1% PEG400, and 1−2% DMSO at 25.0 or 26.0 ± 0.1 °C

P_3-P_2-P_1 + P_1'-P_2'-P_3'	10^6K_M (M)	k_{cat} (s^{-1})	k_{cat}/K_M (M^{-1} s^{-1})
PR-AMC	262 ± 11	1.3 ± 0.1	(5.1 ± 0.1) × 10^3
VPR-AMC	9.3 ± 0.3	73.8 ± 0.8	(7.9 ± 0.1) × 10^6
SPR-SFE	36.6 ± 1.7	54.2 ± 1.6	(1.5 ± 0.1) × 10^6
FPR-SFR	260 ± 35	2336 ± 225	(9.0 ± 0.4) × 10^6
FVR-pNA[a]	130 ± 20	25 ± 8	(2.0 ± 0.6) × 10^5
FP_iR-pNA[b]	(3)	95 ± 20	(4 × 10^7)

[a] 0.03 M NaCl. [b] 37.0 ± 0.2 °C; values in parentheses are from AB Kabi manufacturer's literature.

pH-Dependence and Proton Inventory Experiments. The pH dependence of the thrombin-catalyzed hydrolysis of (AB)Val-Phe-Pro-Arg-Ser-Phe-Arg-Leu-Lys(DNP)-Asp-OH and (AB)Val-Ser-Pro-Arg-Ser-Phe-Gln-Lys(DNP)-AspOH was followed under pseudo-first-order conditions at 0.8−5 μM and fixed enzyme concentration for 4−5 half-lives. Michaelis−Menten studies were performed in the range pL 7.1−9.6 (L = H, D) at 15−20 substrate concentrations between 0.15 and 15 K_m, except for the fluorescence-quenched substrates and Bz-Val-Phe-Arg-pNA when substrate solubility limited the applicable concentrations to 1.5−3.5 K_m. Proton inventory studies were performed at pH 8.3−8.5 and equivalent pL in isotopic buffers at $n = 0-1$ using either initial rates or at [S] ≪ K_m under pseudo-first-order conditions, in three repeats. No deviation from pseudo-first-order was observed at >95% completion of the reaction. The same thrombin stock solution diluted to between 1 and 50 nM was used for a set of pH or proton inventory study; it maintained activity for long working days.

Kinetic Measurements. In all measurements, the enzyme solution was added from an aqueous solution in 0.5−1% of the total volume of 1.00 mL for spectrophotometric measurements and 2.35 mL for spectrofluorometric measurements to the buffer in a cuvette and was prethermostated for 10−15 min at the working temperature. The reaction was initiated by the injection of 20−22 μL of substrate solution in DMSO. Initial rates of substrate hydrolysis were calculated from 100 to 1000 fluorescence intensities or absorbance readings at 400 nm in 1 min. Pseudo-first-order measurements of k_{cat}/K_m were also performed according to this protocol.

Analysis of Kinetic and Proton Inventory Data. All data reductions using predefined and custom-defined equations were performed using the GraFit 3.3 software.[43]

Results

Classic Michaelis−Menten kinetics was observed in all cases. Table 1 summarizes the kinetic parameters calculated from initial rate measurements.

Substrate quenching of products released were observed at high concentrations with *Z*-Pro-Arg-7-AMC and (AB)Val-Ser-Pro-Arg-Ser-Phe-Gln-Lys(DNP)-Asp-OH. These were studied, and calibration curves were constructed to correct for quenching of intensities at high substrate concentrations. A sample calibration curve is shown in Figure 1.

The Michaelis−Menten constants for the thrombin-catalyzed hydrolysis of substrates were characterized as a function of pH and dependence on cosolvent and NaCl concentrations. Figure 2 demonstrates typical pH dependences of k_{cat}/K_m for the hydrolysis of *N*-*t*-Boc-Val-Pro-Arg-7-AMC. k_{cat} was pH independent.

The data were fit to $k_{cat}/K_m = k_{lim1}K_a/(K_a + [H^+])$, and the obtained values of K_as were 7.45 ± 0.03 in water and 7.96 ± 0.04 in D_2O. p*K* values within ±0.1 of 7.45 were obtained for other cases. A possible second p*K* above 8.5 was not characterized. Ratios of rate constants measured in mixed isotopic solvents, at the pL plateau, over rate constants measured in water, were plotted against the atom fraction of deuterium, *n*, in the buffer, shown in Figures 3−8. Proton inventories were also constructed for the hydrolysis of internally fluorescence-quenched peptides under pseudo-first-order conditions at substrate concentrations at 0.2 K_m. The results from these measurements were in good agreement with the proton inventory data obtained from full Michaelis−Menten studies. Initial rates were measured at substrate concentrations ∼10 K_m for *H*-D-Phe-L-Pip-Arg-pNA. Bz-Phe-Val-Arg-pNA has a limited solubility under the experimental conditions at ∼3 × 10^{-4} M (4 K_m). To maximize enzyme saturation with this substrate, the salt level was kept below optimal[39,44] (0.3 M) at 0.03 M NaCl.

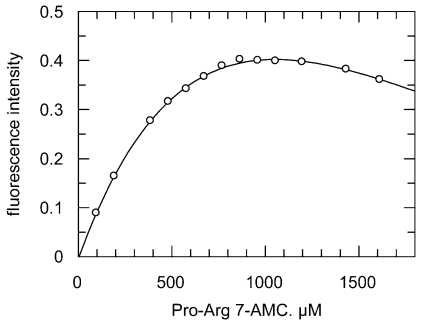

Figure 1. Fluorescence quenching by increasing the concentration of *Z*-Pro-Arg-7-AMC at pH 8.43 and 26.0 ± 0.1 °C.

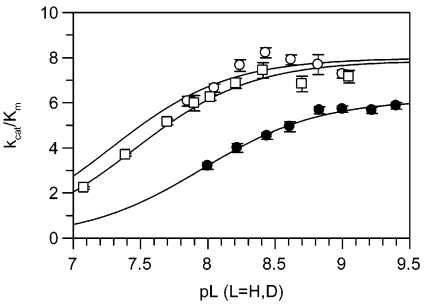

Figure 2. pH-Dependence of the Michaelis−Menten constants for the human α-thrombin-catalyzed hydrolysis of *N*-*t*-Boc-Val-Pro-Arg-7-AMC in 0.02 M Tris, 0.3 M NaCl, 0.1% PEG-4000 at 25.0 ± 0.1 °C. Circles: 1% DMSO; open, L = H; filled, L = D. Squares: 2% DMF; L = H.

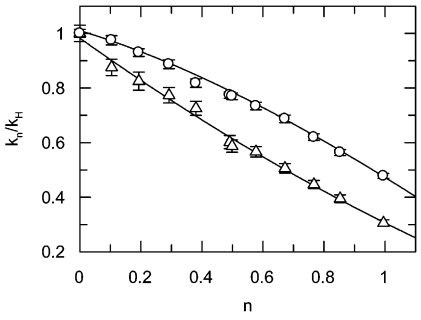

Figure 3. Proton inventory for the human α-thrombin-catalyzed hydrolysis of *Z*-Pro-Arg-7-AMC in 0.02 M Tris buffer containing 0.3 M NaCl, 1% DMSO, and 0.1% PEG-4000 at 26.0 ± 0.1 °C. Circles represent k_{cat}/K_m, and triangles are for k_{cat}. Curves have been calculated from best-fit models outlined in Chart 1.

(43) Leatherbarrow, R. J. *GraFit User's Guide*; Ertihacus Software Ltd.: Staines, U.K., 1992.

(44) Di Cera, E.; Guinto, E. R.; Vindigni, A.; Dang, Q. D.; Ayala, Y.; Wuyi, M.; Tulinsky, A. *J. Biol. Chem.* **1995**, *270*, 22089−22092.

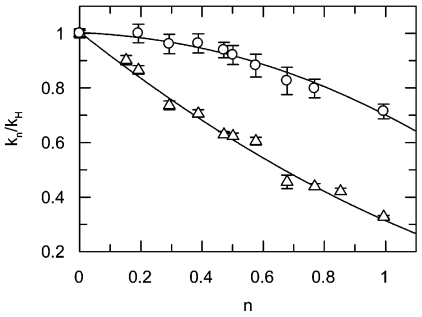

Figure 4. Proton inventory for the human α-thrombin-catalyzed hydrolysis of *N*-*t*-Boc-Val-Pro-Arg-7-AMC; conditions and symbols are as those in Figure 3.

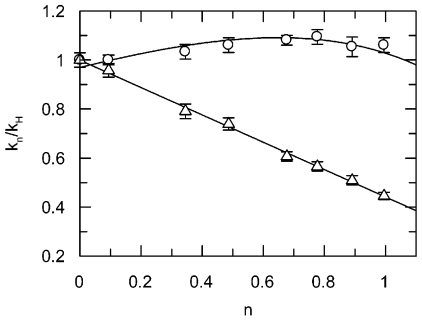

Figure 5. Proton inventory for the human α-thrombin-catalyzed hydrolysis of (AB)Val-Ser-Pro-Arg-Ser-Phe-Gln-Lys(DNP)-Asp-OH; conditions and symbols are as those in Figure 3.

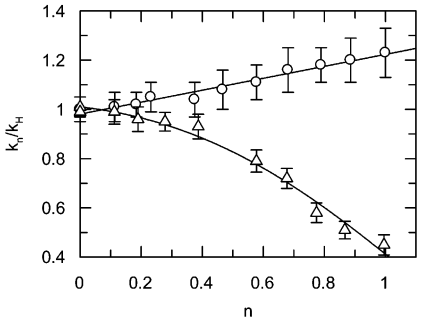

Figure 6. Proton inventory for the human α-thrombin-catalyzed hydrolysis of (AB)Val-Phe-Pro-Arg-Ser-Phe-Arg-Leu-Lys(DNP)-Asp-OH; conditions are as those in Figure 3. Circles are for pseudo-first-order rate constants, and triangles are for k_{cat}.

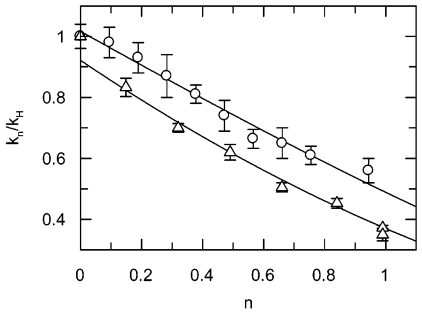

Figure 7. Proton inventory for the human α-thrombin-catalyzed hydrolysis of Bz-Phe-Val-Arg-pNA in 0.02 M Tris buffer containing 0.03 M NaCl, 2% DMSO, and 0.1% PEG-4000 at 25.00 ± 0.05 °C. Circles are for pseudo-first-order rate constants, and triangles are for k_{cat}.

Evaluation of Proton Inventory Data and Selection of a Model. The Gross−Butler equation,[11,12,15,45,46] given below,

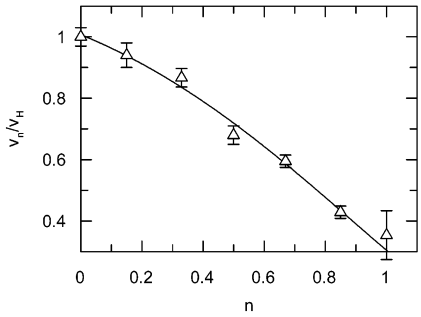

Figure 8. Proton inventory for the human α-thrombin-catalyzed hydrolysis of *H*-D-Phe-L-Pip-Arg-pNA in 0.02 M Tris buffer containing 0.3 M NaCl, 2% DMSO, and 0.1% PEG-4000 at 37.0 ± 0.1 °C.

relates the dependence of a particular rate parameter to the atom fraction of deuterium, *n*, in the solvent mixtures,

$$V_n = V_o \prod_i^{TS}(1 - n + n\phi^T{}_i)/\prod_j^{RS}(1 - n + n\phi^R{}_j) \qquad (1)$$

where V_n and V_o are velocity (or rate constant) in a binary solvent and in water, respectively, n = atom fraction of deuterium, RS = reactant state, ϕ^R = RS fractionation factor, and ϕ^T = TS fractionation factor. The TS product is over TS fractionation factors, and the RS product is over RS fractionation factors. The fractionation factors are in essence inverse equilibrium isotope effects, K_D/K_H, for exchange between a bulk water site and a particular structural site of RS or TS. By a process of least-squares fitting to eq 2, the contributing $\phi^T{}_i$ and $\phi^R{}_i$, i.e., isotope effects, can be obtained. The most common simplifications of this equation involve the assumption of a unit fractionation factor of RSs for catalytic residues with NH and OH functional groups and the assumption that one or two active-site units contribute in most hydrolytic enzymes, resulting in (a) $V_n = V_o(1 - n + n\phi^T)$ or (b) $V_n = V_o(1 - n + n\phi^T{}_1)(1 - n + n\phi^T{}_2)$, respectively. More complex models can also be derived from the general expression.[11−13,15,47] As the up-bulging curves for the dependence of the k_{cat}/K_m isotope effects on n suggest, two opposing trends are prevailing: one with a normal isotope effect and the other with an inverse isotope effect. Admitting past evidence for a strong contribution of solvent reorganization at the TS for this term,[48] while striving for the fewest constraints necessary to obtain the best fit, we calculated a single exponential term for a generalized solvent rearrangement,[12,19] symbolized by $\phi_S{}^n$, regardless of its origin. An alternative model for convex proton inventories assuming change in the rate-determining step gave erratic results with poor statistics. Therefore, we allowed for hydrogen bridges with the solvent contributing to the proton inventory for k_{cat} for the decapeptide and *H*-D-Phe-Pip-Arg-pNA. Models that gave reasonable fit and were deemed feasible in this study are given below in Chart 1.

As suggested above, V_n and V_H represent velocities; alternatively, a phenomenological rate constant, k_{cat}, k_{cat}/K_m, or k_{obs} obtained from a progress curve, can be substituted.

Table 2 shows selected numerical data for the most plausible models used for the proton inventory study of *N*-*t*-Boc-Val-Pro-Arg-7-AMC, which gave the best statistical results as

(45) Gold, V. *Adv. Phys. Org. Chem.* **1969**, *7*, 259−331.
(46) Kresge, A. J. *Pure Appl. Chem.* **1964**, *8*, 243−258.
(47) Schowen, R. L.; Schowen, K. B. *Methods Enzymol.* **1982**, *87*, 551−606.
(48) Stein, R. L. *J. Am. Chem. Soc.* **1985**, *107*, 6039−6042.

Chart 1. Models for Fitting Proton Inventory Data

Information obtained	Equation
TS_1	$V_n = V_H (1 - n + n \phi_1)$
TS_1, solv.	$V_n = V_H (1 - n + n \phi_1) \phi_S^n$
$2TS_1$	$V_n = V_H (1 - n + n \phi_1)^2$
$2TS_1$, solv.	$V_n = V_H (1 - n + n \phi_1)^2 \phi_S^n$
TS_1, TS_2	$V_n = V_H (1 - n + n \phi_1)(1 - n + n \phi_2)$
TS_1, TS_2, solv.	$V_n = V_H (1 - n + n \phi_1)(1 - n + n \phi_2) \phi_S^n$
TS, RS	$V_n = V_H (1 - n + n \phi_1)/(1 - n + n \phi_R)$

Table 2. Fractionation Factors Fitting Various Models[a] for the Hydrolysis of *N*-*t*-Boc-Val-Pro-Arg-7-AMC Catalyzed by Human α-Thrombin at pH 8.45, 0.02 M Tris buffer, 0.3 M NaCl, 1% DMSO, 0.1% PEG-4000 at 26.0 ± 0.1 °C (Data Were Fit Using Explicit Weighting by Incorporating Individual Errors)

	ϕ_1	ϕ_2	ϕ_S	χ^2
		k_n/k_H		
TS_1	0.32 ± 0.01			4.997
TS_1, solv	0.44 ± 0.05		0.70 ± 0.10	2.526
$2TS_1$	**0.57 ± 0.01**	**0.57 ± 0.01**	**(1.00)**	**2.278**
$2TS_1$, solv	0.56 ± 0.04	0.56 ± 0.04	1.04 ± 0.15	2.514
TS_1, TS_2	0.49 ± 0.15	0.66 ± 0.20	(1.00)	2.515
		$(k_{cat}/K_M)_n/(k_{cat}/K_M)_H$		
TS_1	0.73 ± 0.03			1.335
TS_1, solv	0.42 ± 0.03		1.65 ± 0.10	0.274
$2TS_1$	0.86 ± 0.02	0.86 ± 0.02	(1.00)	1.514
$2TS_1$, solv	**0.55 ± 0.02**	**0.55 ± 0.02**	**2.4 ± 0.2**	**0.236**
TS_1, TS_2	0.47 ± 0.02	1.50 ± 0.06	(1.00)	0.222

[a] Most consistent model is denoted in boldface.

measured by the reduced χ^2. The fractionation factors calculated with the model of choice, based on the goodness of fit and a consistent and sensible mechanism, are printed in bold face letters, and Figure 4 shows the proton inventory curve. For example, consistent with the expectation that acylation is the rate-determining chemical step under k_{cat} as well as k_{cat}/K_m conditions, we found almost identical fractionation factors for the two-proton bridge plus solvation model for k_{cat} and k_{cat}/K_m. In both cases, we obtained the lowest reduced chi squared when no more than two parameters were calculated. There are some insignificant differences in the reduced chi squared values, but only one model offers consistent and plausible fractionation factors. For k_{cat}, fractionation factors for TS_1 and TS_2 are 0.56−0.57 (isotope effect = 1.9 for each proton bridge), when they are constrained to be equal, whether ϕ_S is calculated or constrained to 1.0, because it is 1.0 within experimental error. There is a slight difference between the two fractionation factors when the contribution of solvent is constrained to 1.0, but ϕ_1 and ϕ_2 are not constrained to be equal. Nearly the same value, 0.55, is obtained for the k_{cat}/K_m term when the values of ϕ_1 and ϕ_2 are constrained to be equal, but ϕ_S is calculated. Actually the reduced chi squared is only slightly lower when ϕ_1 and ϕ_2 are free to take any values, while ϕ_S is set to 1.0, but this model is in disagreement with the best model for k_{cat}. Overall the data are consistent with two protons participating in either the formation or breakdown of the tetrahedral adduct in the rate-determining acylation. Solvent reorganization occurring at the TS for acylation masks the contribution of the proton-transfer steps under k_{cat}/K_m conditions in the overall KSIE, but the proton inventory analysis aids in unraveling the contribution and nature of elementary steps.

All KSIEs and fractionation factors obtained from the best-fitting model for each set of proton inventory data are summarized in Table 3. These parameters were used for calculating the curves in Figures 3−8.

Discussion

Choice of Substrates and Significance of Subsite Interactions. To elucidate protonic participation at the rate-determining TS for catalysis by thrombin, we targeted a series of substrates from the simplest amides, *Z*-Pro-Arg-7-AMC, which meets the requirement for the P_1 and P_2 sites, to peptides of increasing size and complexity. Since measurements were performed at the plateau of the pL-rate profile for the parameter to be characterized, the conditions and the substrates only mimic the physiologically optimal. Na^+, the most important modulator of thrombin, promotes a conformational change to the so-called "fast" form, which is operational for the activation of fibrinogen.[41,44,49,50]

Thrombin-catalyzed hydrolysis of substrates that probe the P−S subsite interactions have been good mechanistic tools in a number of investigations. The Michaelis−Menten kinetic constants measured (Table 1) for the oligopeptides-AMC substrates are slightly smaller than those reported for analogous or similar pNA substrates. Some k_{cat}/K_m values approach 10^8 M^{-1} s^{-1} reported for k_1, the rate constant for association of the best substrates with thrombin.[40] Clearly, the effect of a fitting residue at the S_3 site is great on the magnitude of both k_{cat} and k_{cat}/K_m. The two substrates containing key P_1'−P_3' subsites have not been studied earlier. It is somewhat surprising that the decapeptide substrate apparently binds as poorly as the dipeptidyl-AMC, which may be a result of a compromised accommodation of probably the leaving group segment. This, however, is compensated for by a high k_{cat} value and the (related) bimolecular rate constant for encounter, so association of thrombin with the decapeptide occurs at near the highest rate.

The pK_a values calculated for the free enzyme from the pH dependence of k_{cat}/K_m are similar to those for Arg-containing

Table 3. Summary of KSIE and Fractionation Factors (TS, ϕ; Solvent, ϕ_S) for the Human α-Thrombin-Catalyzed Hydrolysis of Peptide Substrates at pH 8.40, 0.02 M Tris Buffer, 0.3 M NaCl, 1% PEG-4000, and 1−2% DMSO at 25.0 or 26.0 ± 0.1 °C

P_3-P_2-P_1 + P_1'-P_2'-P_3'	$^{DOD}k_{cat}$	ϕ_1; ϕ_S	$^{DOD}(k_{cat}/K_M)$	ϕ_1; ϕ_S
PR-AMC	3.27 ± 0.13	0.38 ± 0.05;0.8 ± 0.1	2.09 ± 0.04	0.38 ± 0.02; 1.22 ± 0.04
VPR-AMC	3.05 ± 0.05	$(0.57 \pm 0.01)^{2a}$	1.40 ± 0.05	$(0.55 \pm 0.02)^{2a}$; 2.4 ± 0.2
	or	0.44 ± 0.05; 0.7 ± 0.1		0.42 ± 0.03;1.6 ± 0.1
PR-SF	2.24 ± 0.08	0.44 ± 0.01	0.94 ± 0.03	0.44[b]; 2.4 ± 0.05[c]
FPR-SFR	2.25 ± 0.24	$(0.36 \pm 0.04)^{2a}$; 3.1 ± 0.5	0.81 ± 0.08	- -[d]; 1.24 ± 0.02[e]
FVR-pNA	2.86 ± 0.06	$(0.63 \pm 0.02)^{2a}$	1.8 ± 0.1	$(0.63)^{2ab}$; 1.2 ± 0.04[e]
FP_iR-pNA	2.86 ± 0.07	$(0.40 \pm 0.05)^{2a}$; 2.0 ± 0.4	1.0 ± 0.2	- -; - -

[a] Two identical fractionation factors. [b] Constrained to this value. [c] k_{cat}/K_m data supported by pseudo-first-order kinetic data. [d] Not calculated. [e] Pseudo-first-order kinetic data.

substrates. The activity of thrombin for these substrates declines above pH 8.5, probably due to the effect of Arg ionizing. An upper p$K_a \approx 8.6-9.0$ was assigned to Ilu16, which holds Asp194 in a salt bridge as a result of zymogen activation.[51]

Rate-Determining Step in the Target Reactions: Origin of Solvent Isotope Effects. The acylation manifold is generally slower than deacylation in the hydrolysis of amides and peptides catalyzed by serine proteases.[1,2,5] Hence, proton bridging occurring concurrently with either C−O bond formation to Ser[195] and/or bond cleavage to the leaving group in the tetrahedral intermediate is the focus of these investigations. The Michaelis−Menten parameters, in terms of elementary rate constants, simplify to $k_{cat}/K_m = k_1k_2/(k_{-1} + k_2)$ and $k_{cat} = k_2$, when $k_2 < k_3$. Solvent isotope effects greater than 2 result from primary hydrogen isotope effects, including when proton bridges, i.e., SSHBs, are formed at the TS of the rate-determining step.[4] In evolutionarily highly developed enzymes, there is a great commitment[52−54] to catalysis ($C_f = k_2/k_{-1} > 1$; $C_{Vf} = k_2/k_3 < 1$ in Scheme 2), and thus, the rate-determining step of naturally occurring reactions and their mimics is often near diffusion control under low substrate concentration. The isotopically sensitive steps would then be "masked" by rate-determining association, i.e., $k_{cat}/K_m = k_1$. A small solvent isotope effect, ∼1.17, is expected due to diffusion.[13] Conformational changes can be associated with inverse isotope effects that are essentially the product of many small effects but can add up to significant values (0.3−0.9).[48] In these cases, the barrier(s) to the chemical step(s) can be raised by the addition of cosolvent[13,40,50,55] or salts[41,50,56] to disfavor the reaction by the electrostatic milieu or by changing the temperature.[41,50,56] Using this technique, fibrinogen activation to fibrin 1 and FpA and the second step, formation of fibrin and FpB, have been shown[41] to be ∼67% limited by the chemistry of acylation and ∼33% by the encounter step ($\Delta\Delta G^{TS} = 0.4$ kcal/mol) at pH 8.0, $Na^+ > 0.2$ M, and 37 °C. Similar studies showed that at low substrate concentrations an isotopically insensitive step is partly rate limiting in the thrombin-catalyzed hydrolysis of Ac-D-Phe-Pip-Arg-pNA and to a lesser extent of Tos-Gly-Pro-Arg-pNA.[40] In these cases, KSIE values are typically less than 2, and proton inventory studies deem promising for dissecting the overall KSIE into intrinsic isotope effects, due to the contribution of protons participating in catalysis and hydrogen bonds in solvates that rearrange at the TS. Indeed, the KSIEs for k_{cat}/K_m of most reactions of this study have a component of each isotopically more and less sensitive steps. KSIEs for k_{cat} have so far been observed between 1.5 and 4 and generally without contribution of solvent rearrangements.[4,11] However, all earlier reports pertain to substrates with small leaving groups. The situation changes with *H*-D-Phe-Pip-Arg-pNA and the decapeptide substrate of thrombin that has a long leaving group fragment.

Dissection of Solvent Isotope Effects into Isotopically Sensitive and Less-Sensitive Sites. Summarized in Table 3, KSIEs for k_{cat} are near 3 with simple fluorogenic and chromogenic substrates and 2.2 ± 0.2 for two intramolecularly fluorescence-quenched substrates. The fractionation factors for k_{cat} and k_{cat}/K_m for the rate-determining chemical step in acylation of thrombin by the substrates studied are identical within experimental error. The intrinsic KSIEs are between 1.7 and 2.8 in thrombin-catalyzed reactions. The proton inventory data for the hydrolysis of the decapeptide are the most complex, they fit only an exponential function giving $\phi_S = 1.24 \pm 0.02$ at low substrate concentration and $\phi^{TS}_1 = \phi^{TS}_2 = 0.68 \pm 0.02$ plus a large inverse component, $\phi_S = 3.1 \pm 0.5$, at high substrate concentration. Clearly, the rate-determining steps are different under the two conditions; it is probably association at low substrate concentration and C−N bond breaking including leaving group dissociation under high substrate concentration.

A single-proton bridge at the TS and solvent rearrangement gives the most consistent model for the hydrolysis of *Z*-Pro-Arg-AMC, with a small value of ϕ_S for k_{cat} and a larger one for k_{cat}/K_m. Since the ratio $[(k_{cat}/K_m)_n/(k_{cat}/K_m)_H]/[(k_{cat})_n/(k_{cat})_H] = (K_m)_H/(K_m)_n = \phi_S^{V/K}/\phi_S^{V} = 1.22/0.8 = 1.5$ gives the solvent isotope effect for K_m, the dissociation of the substrate from thrombin due to solvent reorganization; its inverse, 0.67, is the solvent isotope effect for association. Solvent rearrangement contributing to the KSIE for k_{cat} ($\phi_S = 0.8$) probably occurs during rate-determining C−O bond formation with this short substrate.

Although Pro is the preferred residue at the S_2 site, when Pro, Val, or Pip occupies the S_2 site in the tripeptide amides, two protons participate in the rate-determining catalytic process. Conventional wisdom dictates that the two-proton bridges be assigned to those in the catalytic triad; the participation of other catalytic residues has been essentially precluded.[3,11,15,16,47] The possibility of the participating hydrogen bridges at the TS originating from the hydrogen bonds in the oxyanion hole emerged in the past,[18] since these contribute to the catalytic power of serine hydrolases with 6−8 kcal/mol stabilization of the TS. However, experimental evidence using subtilisin mutants without the hydrogen-bond donors of the oxyanion hole did not support this possibility.[19]

The proton inventory for k_{cat} obtained with the nonapeptide substrate gives the best fit with the single-proton-bridge model. This is somewhat perplexing, when providing only the appropriate P−S interactions can elicit two-proton bridges at the TS. Perhaps the presence of $P_1'-P_5'$ residues disrupts the correct alignment, at least in the absence of other external-site interactions, which may have corrective effects on misfits. Linearity can also be fortuitous, caused by canceling effects of normal and inverse isotope effect components.[3,12,19] In agreement with previous studies, proton inventories for k_{cat} for three substrates show no indication of solvent reorganization being part of the rate-determining process and $\phi_S = 0.8 \pm 0.1$ for k_{cat} of the hydrolysis of *Z*-Pro-Arg-pNA. Proton inventory for k_{cat} of the decapeptide substrate, containing the Phe-Pro-Arg-Ser-Phe-Arg sequence, gives a domed curve with the best statistical fit to a model of two TS sites plus solvation term. Whereas this outcome is in line with the tripeptide substrates, the solvation term yields an intrinsic KSIE of 0.31 ($\phi_S = 3.1 \pm 0.5$) consistent with a conformational rearrangement, which involves a major solvent

(49) Ayala, Y.; Di Cera, E. *J. Mol. Biol.* **1994**, *235*, 733−746.
(50) Wells, C. M.; Di Cera, E. *Biochemistry* **1992**, *31*, 11721−11730.
(51) Mathur, A.; Schlapkohl, W. A.; Di Cera, E. *Biochemistry* **1993**, *32*, 7568−7573.
(52) Cleland, W. W. *CRC Crit. Rev. Biochem.* **1982**, *13*, 385−427.
(53) Cleland, W. W. Enzyme Kinetics as a Tool for Determination of Enzyme Mechanisms. In *Investigations of Rates and Mechanisms of Reactions, Part I*; Bernasconi, C. F., Ed.; Wiley: New York, 1986; p 791.
(54) Cleland, W. W. Secondary Isotope Effects on Enzymatic Reactions. In *Isotopes in Organic Chemistry*; Buncel, E., Lee, C. C., Eds.; Elsevier: Amsterdam, 1987; p 61.
(55) Hopfner, K. P.; Di Cera, E. *Biochemistry* **1992**, *31*, 11567−11571.
(56) Di Cera, E.; De Cristofaro, R.; Albright, D. J.; Fenton, J. W. *Biochemistry* **1991**, *30*, 7913−7924.

reorganization. This is also the case with *H*-D-Phe-PiP-Arg-pNA, the most reactive substrate of thrombin in Table 1, which provides the best fit with a solvation term associated with a KSIE of 0.5 ($\phi_S = 2.0 \pm 0.3$). These solvation terms can be attributed to the well-documented conformational adjustment of thrombin, for example, in catalyzing fibrinogen activation.[41,57] C−N bond breaking in the tetrahedral adduct and the release of the first peptide product seem to contribute to the rate-determining process in the hydrolysis of these complex peptides. Perhaps due to the presence of optimal sequences in these two substrates, leaving group departure occurs at the highest barrier in the course of peptide cleavage. Ac-D-Phe-PiP-Arg-pNA has previously been found a sticky substrate, which is now supported by the proton inventory data for *H*-D-Phe-Pip-Arg-pNA. Leaving group departure in these cases entails a net increase in the isotopic fractionation factors for many proton bridges at sites of solvation. Although these are basically isotopically not so sensitive steps, their aggregate totals up to a large inverse effect.

The KSIEs for the k_{cat}/K_m term are between 0.8 and 2.1 and the data mostly present domed proton inventories, because solvent reorganization contributes an inverse component. The KSIEs decrease with the incorporation of key P and P′ sites in the substrates. Conformational adjustments during binding are well-accepted facts of enzyme catalysis, while evidence for solvent rearrangement associated with this step has been brought about only by solvent isotope effect, proton inventory, and thermodynamic studies. Strongly inverse KSIEs and a large negative entropy of activation were also found for the association of an 1-α-protease inhibitor with elastase.[48] As in this example, we attribute the intrinsic KSIEs between 0.4 and 0.8 ($\phi_S = 1.2-2.4$) to solvent restructuring during the encounter between enzyme and substrate followed by binding. This is commensurate with the allosteric nature of thrombin.[39,57,58] In the associative phase, again, a net increase in the isotopic fractionation factors for hydrogen bonds at solvation sites gives a significant cumulative inverse solvent isotope effect.

Proton inventory studies of reactions catalyzed by the blood cascade enzymes have not before been carried out with the exception of the thrombin-catalyzed hydrolysis of the minimum substrate *Z*-Arg-ethyl ester. The rate-determining step for this reaction is, at least partly, deacylation. Not unexpectedly, this reaction involves one-proton catalysis.[59] There was reason to believe that the multi-proton mechanism of serine protease catalysis is an important source of the unusual catalytic power of the blood cascade enzymes with their natural substrates. For example, Lottenberg et al.[60] suggested that the unique pH dependence of the hydrolysis of a series of oligopeptide substrates could be explained by two or three protons participating in the mechanism. Sizable solvent isotope effects were reported by Stone et al.,[40] which lent support to our anticipation of multi-proton bridges participating in thrombin-catalyzed hydrolysis of complex substrates. These were indeed observed in this investigation, but the finding of large inverse isotope effects for solvent rearrangement on molecular associations and dissociation has been unexpected.

(57) Di Cera, E.; Dang, Q. D.; Ayala, Y.; Vindigni, A. *Methods Enzymol.* **1995**, *259*, 127−144.
(58) Di Cera, E.; Hopfner, K.-P.; Dang, Q. D. *Biophys. J.* **1996**, *70*, 174−181.
(59) Quinn, D. M. University of Kansas, 1978.
(60) Lottenberg, R.; Hall, J. A.; Blinder, M.; Binder, E. P.; Jackson, C. M. *Biochim. Biophys. Acta* **1983**, *742*, 539−557.

Summary

The mobilization of hydrogen bridges in thrombin catalysis by specific enzyme effectors that comply with stringent requirements for the P and P′ sites has been studied by proton inventory. Single- or two-proton mechanisms for the rate-limiting acylation of thrombin have been observed, similar to proton inventory results of acylation and predominantly deacylation in the hydrolysis of oligopeptide-*p*-nitroanilide substrates, chosen to satisfy the most critical requirements for binding,[3,11,14−17] catalyzed by chymotrypsin, trypsin, and elastase. The efficiency of peptide cleavage is always greatly dependent on the composition of the peptide at the P_1-P_5 positions. When the specificity requirement is met near the scissile bond, a compression is exerted by the subsite interactions toward the active site to elicit the full catalytic power of a serine protease. This has been manifest in multi-proton catalysis proposed to involve Nε2 of His[57] and the Oγ H of Ser[195] and Nδ1 of His[57] and COOβ- of Asp[102] in thrombin, as in the other cases of proteases, in the rate-determining step(s). Results of these studies also establish the effect of P′ residues in leaving group departure: a conformational change associated with a major rearrangement of the water solvate is the hallmark of these interactions. The net increase in the isotopic fractionation factors for hydrogen bonds at solvation sites in the rate-determining catalytic step, as recruited by interactions at the leaving group binding site or substrate specificity site, complements the finds of investigators of P′-site interactions in catalysis[30,31,33] by and inhibition[32] of proteases. The proton inventory technique has permitted again demonstration of the importance of solvent reorganization in the course of binding and leaving group release.

Acknowledgment. We gratefully acknowledge the technical contributions of Linnea Patt and Hajni Viragh and the financial support of this research from the U.S. National Institute of Health, Grant No 1 R15 HL067754-01.

Supporting Information Available: Eight tables of Michaelis-Menten constants, pseudo-first-order rate constants and their ratios for proton inventories. This material is available free of charge via the Internet at http://pubs.acs.org.

JA0320166